

Long Phase Coherence Time and Number Squeezing of two Bose-Einstein Condensates on an Atom Chip

G.-B. Jo, Y. Shin, S. Will, T. A. Pasquini, M. Saba, W. Ketterle, and D. E. Pritchard*

MIT-Harvard Center for Ultracold Atoms, Research Laboratory of Electronics,

Department of Physics, Massachusetts Institute of Technology, Cambridge, MA 02139, USA

M. Vengalattore, M. Prentiss

MIT-Harvard Center for Ultracold Atoms, Jefferson Laboratory,

Physics Department, Harvard University, Cambridge, MA 02138, USA

(Dated: December 2, 2024)

We measured the relative phase of two Bose-Einstein condensates confined in an radio frequency induced double well potential on an atom chip. We observed phase coherence between the separated condensates for times up to ~ 200 ms after splitting, a factor of 10 beyond the phase diffusion limit expected for a coherent state in our experimental conditions (~ 20 ms). The enhanced coherence time is attributed to number squeezing of the initial state by a factor of 10. In addition, we demonstrated a rotationally sensitive (Sagnac) geometry for a guided atom interferometer by propagating the split condensates.

PACS numbers: 03.75.Dg, 39.20.+q, 03.75.-b, 03.75.Lm

Precision measurements in atomic physics are usually done at low atomic densities to avoid collisional shifts and dephasing. This applies to both atomic clocks and atom interferometers. At high density, the atomic interaction energy results in so-called clock shifts [1], and leads to phase diffusion in Bose-Einstein condensates (BEC) [2, 3, 4, 5, 6, 7]. Most precision measurements with neutral atoms are performed with free-falling atoms in atomic beams [8, 9] or in fountain geometries [10]. Major efforts are currently directed towards atom interferometry using confined geometries, such as atom traps or waveguides, often realized by using atom chips [11]. These geometries are promising in terms of compactness and portability, and also offer the prospect of extending interrogation times beyond the typical 0.5 s achievable in the atomic fountains [10].

However, given the deleterious effects of high atomic density, those devices were thought to be able to operate only at low density and therefore at small flux, seriously limiting the achievable signal-to-noise ratio and sensitivity. Here we show that we can operate BEC interferometer at high density, with mean field energies exceeding $h \times 5$ kHz, where h is Plank's constant. Using an radio frequency (RF) induced beam splitter [13, 14, 15], we demonstrate that condensates can be split reproducibly, so that even after 200 ms, or more than one thousand cycles of the mean field evolution, the two condensates still have a controlled phase. The observed coherence time of 200 ms is ten times longer than the phase diffusion time for a coherent state, i.e., a state with perfectly defined relative phase at the time of splitting. Therefore, repulsive interactions during the beam splitting process [16] have created a non-classical squeezed state with relative number fluctuations ten times smaller than for a Poissonian distribution.

Our work is a major advance in the coherence time of confined atom interferometers, which have operated at interrogation times below ~ 50 ms [13, 17, 18] due to technical limitations. Our work is also advancing the preparation of number squeezed states to much higher atom numbers. Previous experiments in optical lattice [19, 20] and in an optical trap [21] were limited to very small populations ($\sim 1 - 1000$ atoms). In addition, the fact that the clouds could be prepared on an atom chip with dc and RF electric currents, but without any laser beams, is promising for future applications. Finally, we operate the RF induced beam splitter on condensates propagating in an atom chip waveguide realizing a rotationally sensitive (Sagnac) interferometer.

For two separated Bose-Einstein condensates, a state of well-defined relative phase (phase coherent state), $|\phi\rangle$, is a superposition state of many relative number states, $|N_r = N_1 - N_2\rangle$, where N_1 and N_2 are the occupation of each well for $N = N_1 + N_2$ atoms. Because of atom-atom interactions in the condensates, the energy of number states, $E(N_1, N_2)$, have quadratic dependence on the atom numbers N_1 and N_2 so that the different relative number states have different phase evolution rates [2, 5]. A superposition state will therefore have a spread of evolution rates, causing "phase diffusion" or "decoherence" of the relative phase with time. In contrast to normal diffusion processes, the phase uncertainty, $\Delta\phi$, increases here linearly. The phase diffusion rate, R , is proportional to the derivative of the chemical potential of condensates, $\mu(N_i)$ ($i = 1, 2$), with respect to the atom number and the standard deviation of the relative atom number, ΔN_r : $R = (2\pi/h)(d\mu/dN_i)_{N_i=N/2}\Delta N_r$ [2, 3, 4, 5, 6, 7]. A number squeezed state with sub-Poissonian number fluctuations ($\Delta N_r = \sqrt{N}/s$), where $s > 1$ is the squeezing factor, will exhibit a reduced phase diffusion rate relative

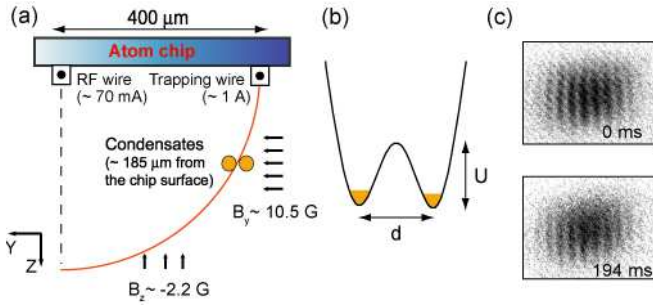


FIG. 1: Schematic of the atom chip interferometer. (a) Atoms were confined radially by the combined magnetic potential of a current-carrying wire and external bias field. Axial confinement in x direction was provided by a pair of endcap wires (not shown) [12]. By dressing the atoms with an oscillating radio frequency (RF) field from a second wire, the single minima in the magnetic trapping potential was deformed into a double-well [13]. If the trapping position lies on the circle containing the trapping wire and centered on the RF wire, the separation of the two wells is in the horizontal plane. Condensates were placed 185 μ m away from the chip surface. For the single well, the radial (axial) trap frequency was $f_r = 2.1$ kHz ($f_z = 9$ Hz) and the Larmor frequency at the trap center was ≈ 190 kHz ($B_x \approx 0.27$ G). Splitting was performed over 75 ms by linearly ramping the frequency of the RF field from 143 kHz to 225 kHz. Gravity points down to $+z$ direction. (b) Double-well potential. The separation d between the two wells and the barrier height U were controlled by adjusting the frequency or amplitude of the RF field. (c) Matter wave interference. For various hold times after splitting, absorption images of condensates released from the double-well potential were taken with 10 ms time-of-flight. The field of view is 260×200 μ m.

to a phase coherent state ($\Delta N_r = \sqrt{N}$).

Bose-Einstein condensates of $\sim 4 \times 10^5$ ^{23}Na atoms in the $|F = 1, m_F = -1\rangle$ state were transferred into a magnetic trap generated by the trapping wire on an atom chip and external bias field[12]. A double-well potential in the horizontal plane was formed using adiabatic RF-induced splitting as described in Fig. 1a [13, 14]. In the typical conditions, the separation of two wells was $d \sim 8.7$ μ m, the height of trap barrier was $U \sim h \times 30$ kHz, and the chemical potential of condensates, measured from the trap bottom, was $\mu \sim h \times 6$ kHz (Fig. 1b). The lifetime of the atoms at the splitting position was ~ 1.8 s, significantly longer than in our previously demonstrated two-wire splitting method [12, 15, 22]. RF-induced splitting has several advantages over two-wire schemes: no loss channel (open port) during splitting, less sensitivity to magnetic bias fields, and realization of high trap frequencies far from a surface [23]. Atoms were held in the double well for varying hold times, released by turning off the trapping potential within 30 μ s at a known phase of the RF field [24], overlapped, and interfered in time-of-flight (Fig. 1c). The relative phase of the two

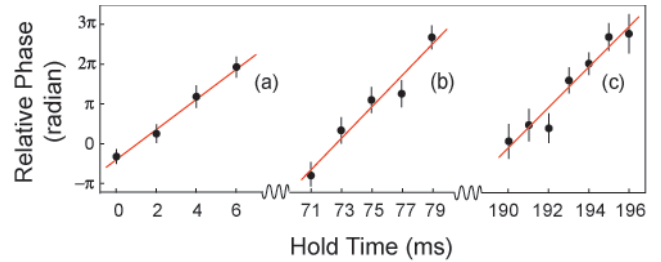


FIG. 2: Phase evolution of the relative phase during three different time intervals. The evolution rate of the relative phase are determined from the linear fit to be (a) 191 Hz, (b) 198 Hz, and (c) 255 Hz. The data points represent the average of ten measurements for (a) and (b), and fifteen for (c).

condensates was measured as the spatial phase of the interference pattern [12, 17].

An atom interferometer requires two independent condensates without any weak link which may lock the phase [12, 17]. To demonstrate this independence, we monitored the relative phase over short intervals from the moment of splitting to 6 ms, from 71 ms to 79 ms, and from 190 ms to 196 ms. During each of these intervals, the phase evolved linearly with time at $\sim 2\pi \times 200$ Hz, the signature of independent condensates (Fig. 2). The slightly different phase evolution rates are attributed to the change in the magnetic potential associated with the axial motion of the separated condensates.

To rule out the possibility that any weak link existed during the 200 ms time evolution and reset the relative phase, we demonstrated that an applied phase shift could be read out 200 ms later. A phase shift was imprinted on the condensates 2 ms after splitting, and the relative phase was measured at 7 ms and 191 ms. The strong correlation between these measurements, shown in Fig. 3, proves that we have created two independently evolving condensates which preserved phase coherence up to 200 ms, a factor of 10 longer than the phase diffusion time, $\tau_c = 1/R \simeq 20$ ms, for our parameters.

For the quantitative study of phase fluctuations, the standard deviation of the phase does not provide the best characterization because the phase is measured modulo 2π . In the limit of a large data set, a completely random distribution has a phase variance of $\sim (3\pi/5)^2$. Already for smaller variances, the overlap of the tails of the Gaussian distribution can cause ambiguities. As a more appropriate measure of correlation, we represent each measurement of the relative phase as a phasor with unit length and compare the length of the sum of N measured phasors with the expectation value of \sqrt{N} for N random phasors. The Rayleigh test compares the phasor sum of the data with the distribution of phasor sums for random data and returns the randomness, the probability that uncorrelated measurements would produce a

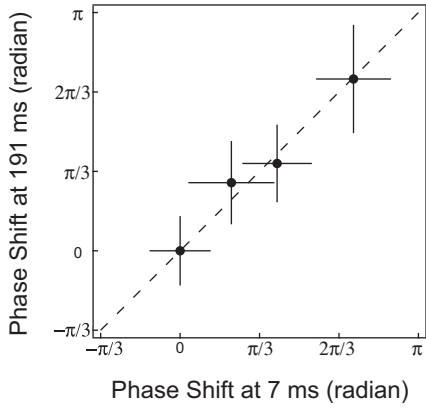


FIG. 3: Long phase coherence of two separated condensates. Applying various phase shifts on the condensates at 2 ms after splitting, the shifts of the relative phase were measured at 7 ms and 191 ms, showing strong correlation. The dotted line denotes the ideal case of perfect phase coherence. Phase shifts of less than 2π were applied by pulsing an additional magnetic field in z direction for 50 μ s with controlled amplitude.

phasor sum larger than the measurement [25]. Uncorrelated data have an expected value of randomness near 0.5, while strongly correlated data would have a small randomness value, e.g. ten data points drawn from a distribution with variance $\pi/5$ have a randomness value near 10^{-4} . If a series of phase measurements has a randomness value of 0.01 (0.1), the relative phase is non-random with a probability of 99% (90%).

To study phase diffusion in our system, we monitor the randomness of ten measurements of the relative phase at various times after splitting, as shown in Fig. 4. The data show a well-defined phase (randomness < 0.1) for times shorter than ~ 200 ms. In contrast, the simulation for a coherent state in our experimental conditions, shown as a blue dotted line, predicts that the randomness climbs above 0.1 at ~ 20 ms. Fitting a phase diffusion rate to the onset of randomness, the red dashed line, gives a phase diffusion time of 200 ms. The solid line is a fit which includes the initial variance $\Delta\phi_0^2$:

$$\Delta\phi(t)^2 = \Delta\phi_0^2 + (Rt)^2 \quad (1)$$

The variance of the initial state, $\Delta\phi_0^2 = (0.28\pi)^2$ is dominated by technical noise including fitting errors and non-ideal trap switch off. The fundamental contribution, $\Delta\phi_0^2 \simeq (s/\Delta N_r)^2$, is $\sim (7.1 \times 10^{-4}\pi)^2$ for a coherent state ($s=1$), and remains small unless the squeezing leads to number fluctuations on the order of a single atom, $s \sim \sqrt{N}$. The fitted value for the phase diffusion rate of $R = 5 \text{ s}^{-1}$ includes technical shot-to-shot variations in the relative atom number of two condensates after splitting. Therefore, the inferred squeezing factor $s=10$ represents a lower bound. It implies that our relative atom number fluctuations were better than $\pm 0.03\%$ cor-

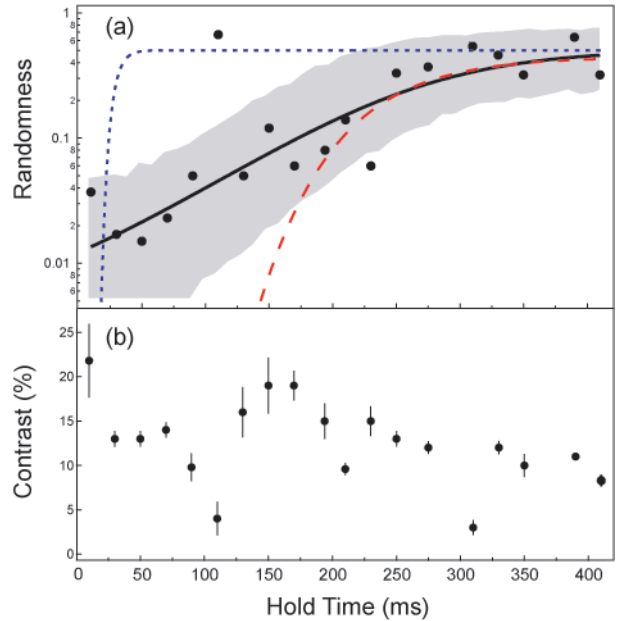


FIG. 4: Phase diffusion and number squeezing. (a) The randomness of ten measurements of the relative phase is displayed up to 400 ms after splitting. The blue dotted curve (red dashed curve) shows the simulated randomness for a phase-coherent state (number squeezed state with $s = 10$), which have negligible initial phase uncertainty. The solid line includes an initial phase uncertainty of 0.28π (see text). The shaded region represents the window where ten data points from the sample with the given phase uncertainty would fall with 50% probability. (b) Contrast of the interference pattern. Since the endcap wires generate a field gradient $\frac{\partial B_z}{\partial x}$ as well as a field curvature $\frac{\partial^2 B_z}{\partial x^2}$ at the position of the condensates, the two wells are not parallel to the trapping wire and consequently have slightly different axial trapping potential. This difference induces relative axial motion of the two condensates, which periodically reduces the contrast.

responding to ± 50 atoms.

Locally the interference pattern of two condensates should always have 100% contrast, where contrast is defined as the density amplitude of the interference fringes over the mean density. Since in our experiment the contrast is derived from interference pattern integrated along the line-of-sight, it decreased gradually with time and exhibited fluctuations most likely due to asymmetric axial motion (Fig. 4b). Except for small regions near 110 and 300 ms hold time, the contrast was above 10%, sufficient for accurate determination of the phase. The small windows with poor contrast have large values of the randomness.

The probable origin of number squeezing during the splitting is repulsive atom-atom interactions [16]. The interactions make it energetically favorable for the two condensates to split with equal numbers in a symmetric double-well potential, whereas a coherent state is a mixture of states with different atom numbers and has higher

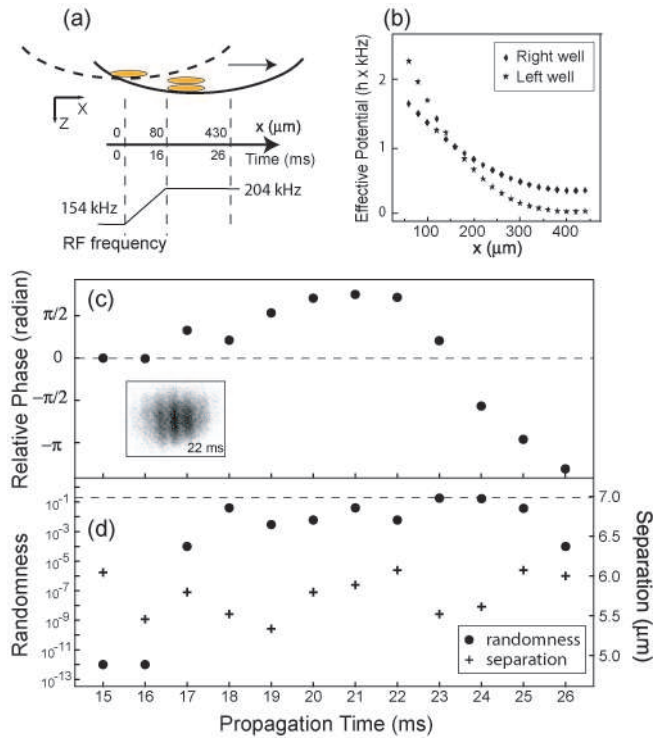


FIG. 5: Guided-atom interferometry with propagating condensates. (a) A single condensate was prepared stationary in a trap with $f_r = 2.1$ kHz and $f_z = 10$ Hz. A dipole oscillation was induced by shifting the trap center by ~ 430 μm in the axial direction ($t = 0$ ms). The frequency of the RF field was linearly ramped from 154 kHz to 204 kHz for 16 ms after launch, splitting the condensates in two parts by $5 - 6$ μm . (b) The effective magnetic potentials of the two wells along the guiding line are calculated for the experiment parameters after splitting, including gravity with an arbitrary offset. (c) Relative phase vs propagation time. For $t \leq 16$ ms, the condensates were not fully separated so that the relative phase was locked, which is indicated by extremely low randomness shown in (d). After splitting ($t > 16$ ms), the two condensates propagated over ~ 300 μm . Due to the effective potential difference of the two wells, the evolution rate of the relative phase was changed from 83 Hz to -261 Hz during propagation. The inset shows the interference pattern for $t = 22$ ms. The field of view is 260×200 μm . (d) The randomness of ten measurements for the relative phase demonstrates phase coherence. The dashed line indicates the full randomness of 0.5. The separation was determined from fringe spacing.

total energy. Therefore, interaction-induced squeezing reduces the phase diffusion caused by the same interactions [26].

A major goal of confined atom interferometry is the development of a rotationally sensitive interferometer, which requires that the two paths of the interferometer have an enclosed area A [8, 9, 27]. A rotation rate Ω then leads to a phase shift $\Delta\phi = [\frac{4\pi m A}{\hbar}]\Omega$, where m is the probe particle mass. This phase shift is due to the Coriolis force and therefore requires moving condensates.

As described in Fig. 5, we were able to accelerate the condensate axially prior to splitting and realized, for the first time, a Sagnac atom interferometer on an atom chip. Propagation distance and time were not limited by the phase decoherence, but by the physical limits of the chip geometry. In this geometry, the area enclosed is ~ 1500 μm^2 , and the response factor $\frac{4\pi m A}{\hbar}$ is $\sim 7.9 \times 10^{-5} \text{ rad}/\Omega_e$, where Ω_e is the earth rotation rate [26]. If the geometry were adjusted to take advantage of the full coherence time of 200 ms, the sensitivity would improve by a factor of 20.

In conclusion, the present work demonstrates a long phase coherence time of ~ 200 ms between two spatially separated condensates on an atom chip, rivaling the interrogation times in fountain-type interferometers [10]. Number squeezing by a factor ≥ 10 occurs during the preparation of the split state, providing a well-defined phase beyond the phase diffusion limit for a coherent state. These results show that it is both possible and promising to use condensates at high density for interferometry on an atom chip.

This work was funded by DARPA, NSF, ONR, and NASA. G.-B. Jo and S. Will acknowledge additional support from the Samsung Lee Kun Hee Scholarship Foundation and the Studienstiftung des deutschen Volkes, respectively. We thank C. Christensen for experimental assistance.

* URL: http://cua.mit.edu/ketterle_group/

- [1] K. Gibble and S. Chu, Phys. Rev. Lett. **70**, 1771 (1993).
- [2] Y. Castin and J. Dalibard, Phys. Rev. Lett. **55**, 4330 (1997).
- [3] M. Lewenstein and L. You, Phys. Rev. Lett. **77**, 3489 (1996).
- [4] E. Wright, D. Walls, and J. Garrison, Phys. Rev. Lett. **77**, 2158 (1996).
- [5] J. Javanainen and M. Wilkens, Phys. Rev. Lett. **78**, 4675 (1997).
- [6] A. Leggett and F. Sols, Phys. Rev. Lett. **81**, 1344 (1998).
- [7] J. Javanainen and M. Wilkens, Phys. Rev. Lett. **81**, 1345 (1998).
- [8] A. Lenef *et al.*, Phys. Rev. Lett. **78**, 760 (1997).
- [9] T. Gustavson, P. Bouyer, and M. Kasevich, Phys. Rev. Lett. **78**, 2046 (1997).
- [10] A. Peters, K. Chung, and S. Chu, Nature **400**, 849 (1999).
- [11] F. Folman *et al.*, Advances in atomic, molecular, and optical physics **48**, 263 (2002).
- [12] Y. Shin *et al.*, Phys. Rev. A **72**, 021604 (2005).
- [13] T. Schumm *et al.*, Nature physics **1**, 57 (2005).
- [14] O. Zobay and B. Garraway, Phys. Rev. Lett. **86**, 1195 (2001).
- [15] Y. Colombe *et al.*, Europhys. Lett. **67**, 593 (2004).
- [16] C. Menotti *et al.*, Phys. Rev. A **63**, 023601 (2001).
- [17] Y. Shin *et al.*, Phys. Rev. Lett. **92**, 050405 (2004).
- [18] O. Garcia *et al.*, cond-mat/0603772 **58**, 1450 (2006).
- [19] C. Orzel *et al.*, Science **291**, 2386 (2001).

- [20] M. Greiner *et al.*, Nature **415**, 39 (2002).
- [21] C.-S. Chuu *et al.*, Phys. Rev. Lett. **95**, 260403 (2005).
- [22] E. Hinds, C. Vale, and M. Boshier, Phys. Rev. Lett. **86**, 1462 (2001).
- [23] I. Lesanovsky *et al.*, Phys. Rev. A **73**, 033619 (2006).
- [24] We observed strong correlation between the population distribution of the spin components and the phase of the RF field at the moment of releasing, probably since the strength of the RF field (~ 0.35 G) was comparable to the local static field (~ 0.24 G) [28]. The trapping potential was switched off at a value of the RF phase chosen to release atoms predominantly in the $|F = 1, m_F = -1\rangle$ state.
- [25] N. Fisher, *Statistical analysis of circular data* (Cambridge University Press, New York, 1993).
- [26] P. Berman, *Atom Interferometry* (Academic Press, New York, 1997).
- [27] M. Sagnac, C.R.Acad. Sci **157**, 708 (1913).
- [28] S. Autler and C. Townes, Phys. Rev. **100**, 703 (1955).